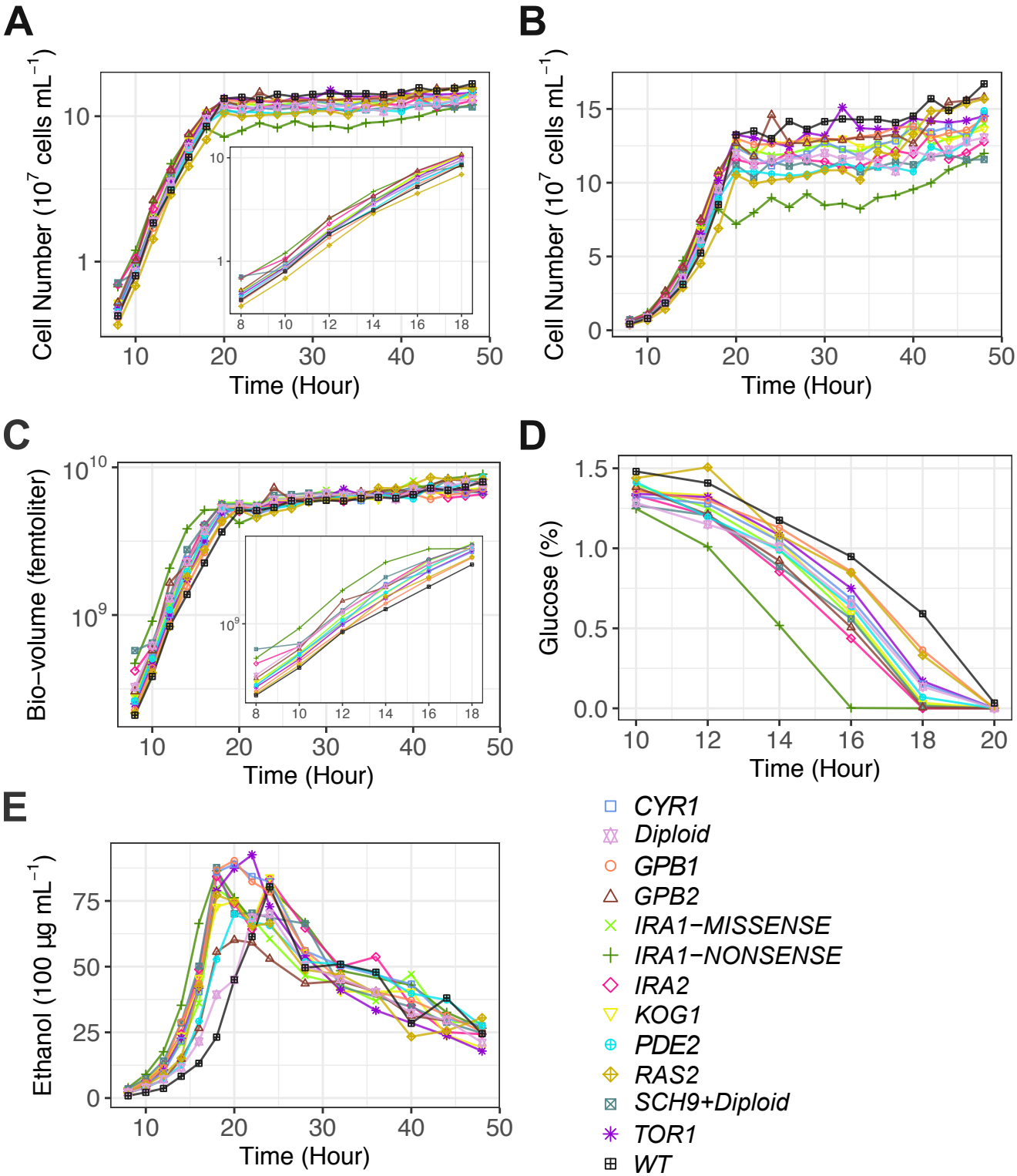
A
Cell Number (10^7 cells mL^{-1})
Time (Hour)
B
Cell Number (10^7 cells mL^{-1})
Time (Hour)
C
Bio−volume (femtoliter)
Time (Hour)
D
Glucose (%)
Time (Hour)
E
Ethanol (100 µg mL^{-1})
Time (Hour)
CYR1
Diploid
GPB1
GPB2
IRA1−MISSENSE
IRA1−NONSENSE
IRA2
KOG1
PDE2
RAS2
SCH9+Diploid
TOR1
WT

Figure S1: Monoculture measurements, Related to Figure 1

Twelve evolved clones and one WT clone were cultured in monocultures under the original evolutionary condition. Growth curves were measured using (A) (B) cell number and (C) bio-volume. (A) shows cell number dynamics in a log scale and (B) shows cell number in a linear scale. The insets in (A) and (C) are the zoom-in of the growth curve during the fermentation phase.

(D) Glucose concentration and (E) Ethanol concentration of the cell cultures were measured across a single growth cycle. Glucose was exhausted around 20h, which gives an estimate for the end of fermentation.

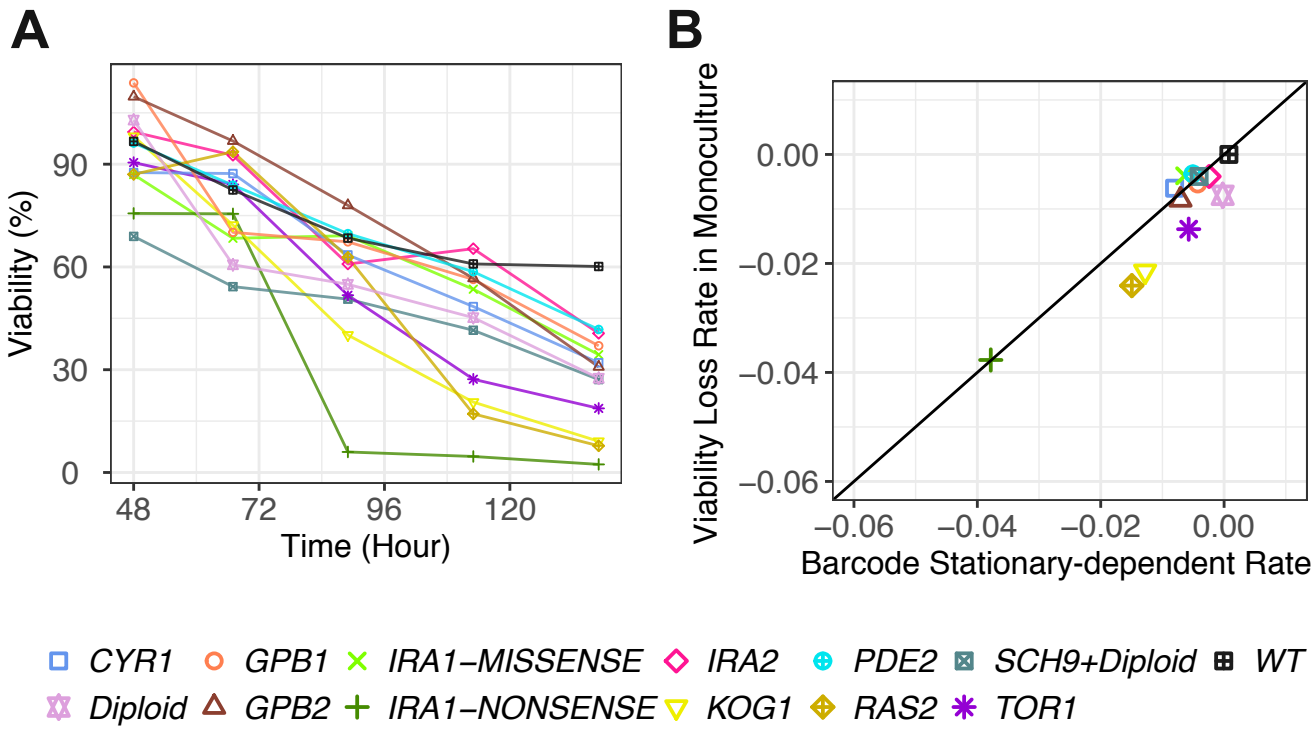
A
Viability (%)
90
60
30
0
48
72
96
120
Time (Hour)
B
Viability Loss Rate in Monoculture
0.00
−0.02
−0.04
−0.06
−0.06
−0.04
−0.02
0.00
Barcode Stationary-dependent Rate
CYR1
GPB1
IRA1−MISSENSE
IRA2
PDE2
SCH9+Diploid
WT
Diploid
GPB2
IRA1−NONSENSE
KOG1
RAS2
TOR1

Figure S2: Viability measurements in monoculture, Related to Figure 5

Twelve evolved clones and one WT clone were cultured in monocultures under the original evolutionary condition. (A) Their viability was tracked from 48h (2 Day) up to 137h (~6 Day).

(B) Relationship between the twelve evolved clones' viability loss rate per hour in monoculture and their stationary-dependent rate estimated from the high-throughput barcode fitness measurements (Pearson's r = 0.92, 95% CI [0.56, 0.98]; R^2 = 0.9). The black line represents y=x.

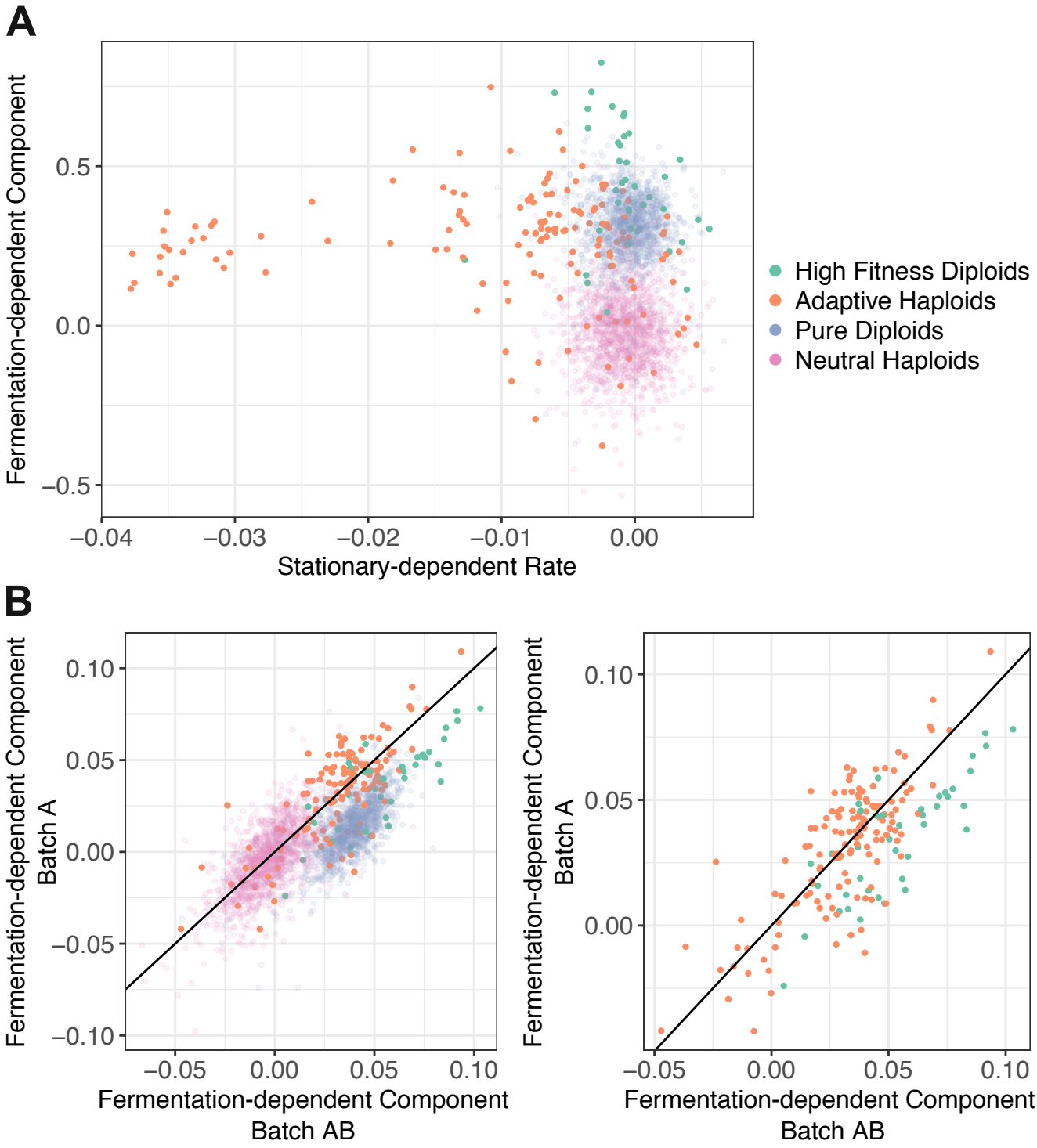
A
Fermentation-dependent Component
0.5
0.0
−0.5
−0.04
−0.03
−0.02
−0.01
0.00
Stationary-dependent Rate
High Fitness Diploids
Adaptive Haploids
Pure Diploids
Neutral Haploids
B
Fermentation-dependent Component
Batch A
0.10
0.05
0.00
−0.05
−0.10
−0.05
0.00
0.05
0.10
Fermentation-dependent Component
Batch AB
Fermentation-dependent Component
Batch A
0.10
0.05
0.00
−0.05
0.00
0.05
0.10
Fermentation-dependent Component
Batch AB

Figure S3: Lack of trade-off between fermentation-dependent component and stationary-dependent rate and fermentation-dependent component estimation, Related to Figure 5

(A) Correlation between the fermentation-dependent component and the stationary-dependent rate estimated from the high throughput barcode fitness measurements (Pearson's r = 0.06, 95% CI [0.01, 0.1] for all adaptive lineages). Each dot represents one evolved lineage and is colored by their ploidy and fitness class under the EC.

(B) Fitness measurements with varying number of generations during fermentation were conducted in two batches: Batch A (4, 6, and 8 generations during fermentation) and Batch B (8 and 9 generations during fermentation). Fermentation-dependent component estimated using measurements from both Batch A and B *vs.* that estimated only using measurements under Batch A. The left panel contains all lineages in the pool with each dot represents a lineage, while the right panel contains only adaptive haploids and high fitness diploids.

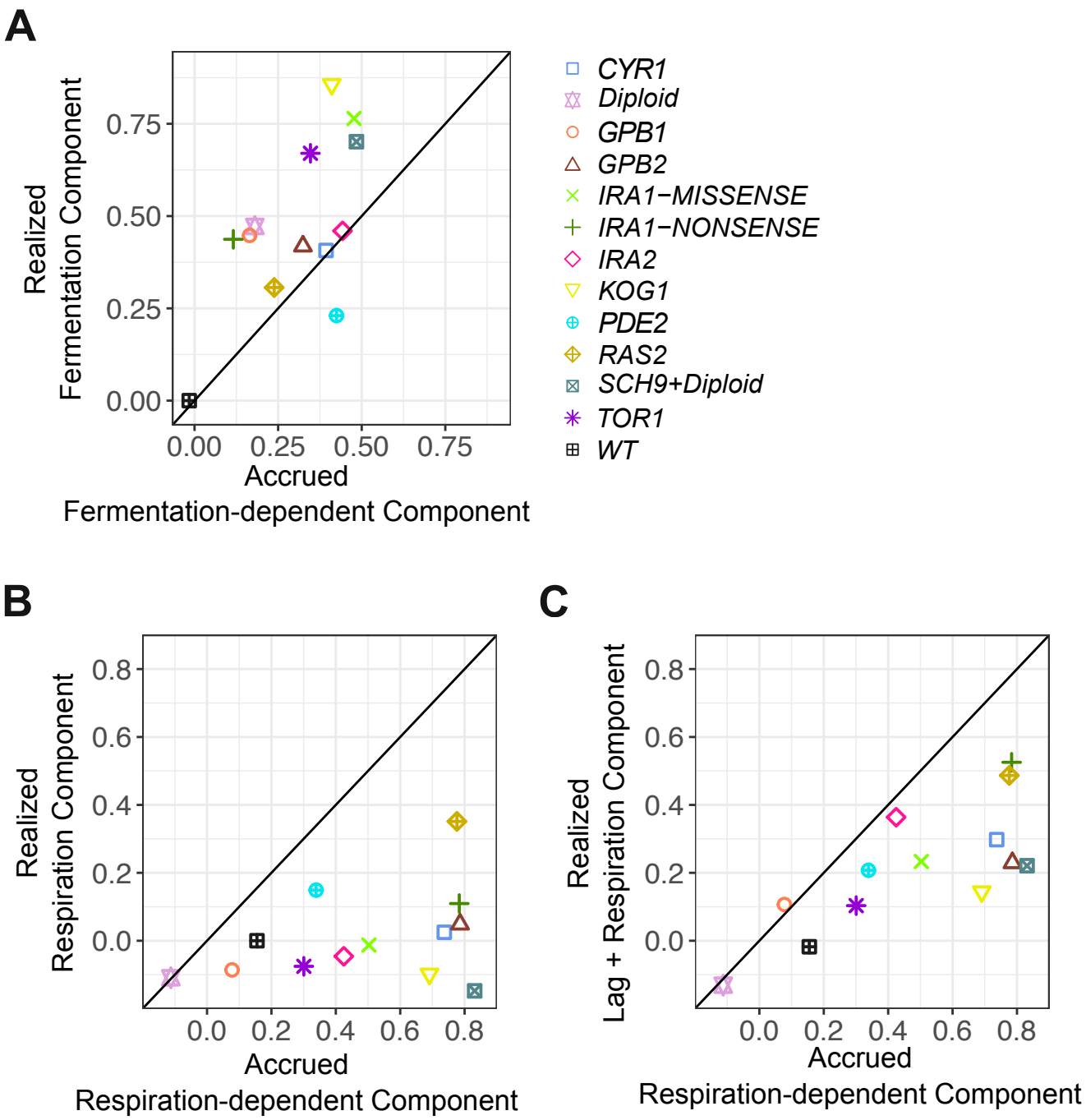
A
Realized
Fermentation Component
0.00
0.25
0.50
0.75
Accrued
Fermentation-dependent Component
CYR1
Diploid
GPB1
GPB2
IRA1−MISSENSE
IRA1−NONSENSE
IRA2
KOG1
PDE2
RAS2
SCH9+Diploid
TOR1
WT
B
Realized
Respiration Component
0.0
0.2
0.4
0.6
0.8
Accrued
Respiration-dependent Component
C
Realized
Lag + Respiration Component
Accrued
Respiration-dependent Component

Figure S4: Comparison of fitness components estimated from different approaches, Related to Figure 6

Comparison of the realized fitness component estimated from the monoculture measurements with the corresponding accrued component estimated from the high-throughput barcode fitness measurements: (A) realized fermentation component from the monoculture measurements with the accrued fermentation-dependent component from the barcode fitness measurements (Pearson's r = 0.66, 95% CI [0.1, 0.91]); (B) realized respiration component from the monoculture measurements with the accrued respiration-dependent component from the barcode fitness measurements; (C) combined realized fitness from the lag and the respiration phases estimated from the monoculture cell number measurements with the accrued respiration-dependent component estimated from the barcode fitness measurements (Pearson's r = 0.75, 95% CI [0.31, 0.92]).

Note, the *ira1-nonsense* mutant is consistently an outlier for each measurement and was excluded from correlation calculations.

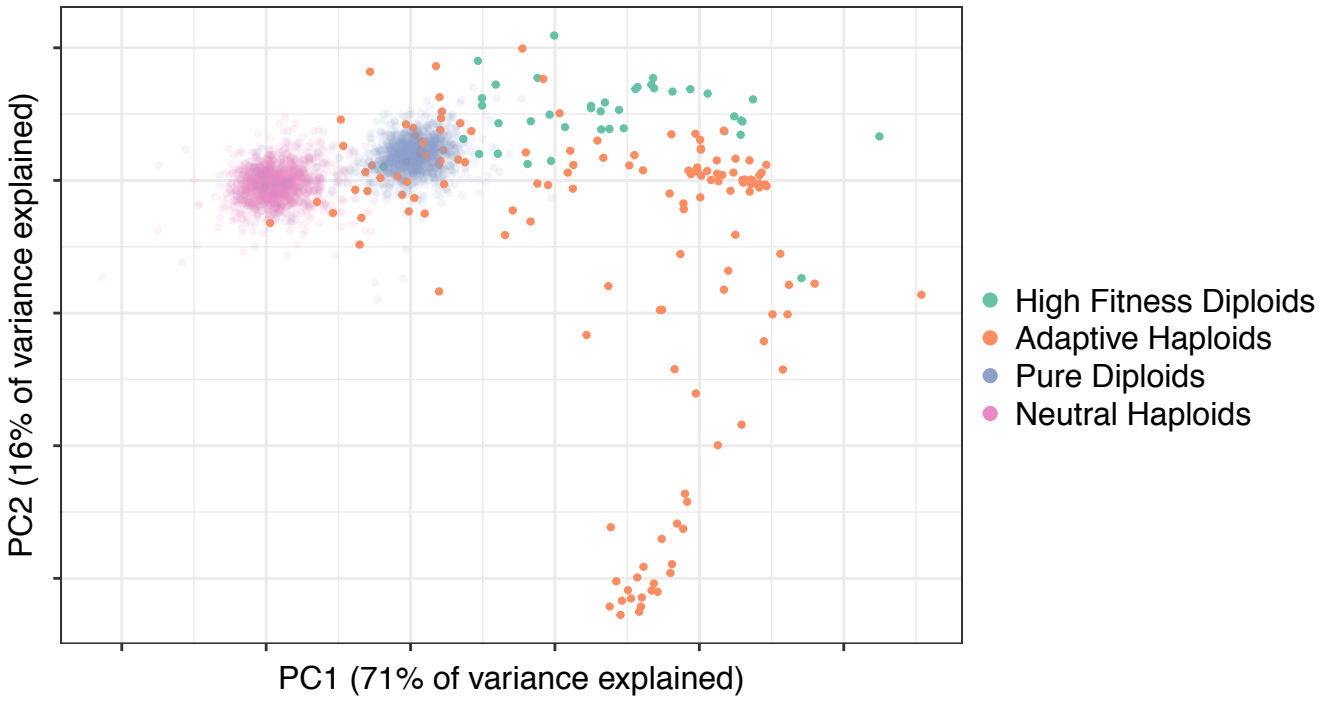
PC2 (16% of variance explained)
PC1 (71% of variance explained)
High Fitness Diploids
Adaptive Haploids
Pure Diploids
Neutral Haploids

Figure S5: PCA analysis using fitness profiles of 3,048 evolved clones, Related to Figure 7

Principal component analysis for all lineages in the pool using their fitness measurements under all test conditions (Figure 3AB). Each dot represents a lineage and is colored by its class.

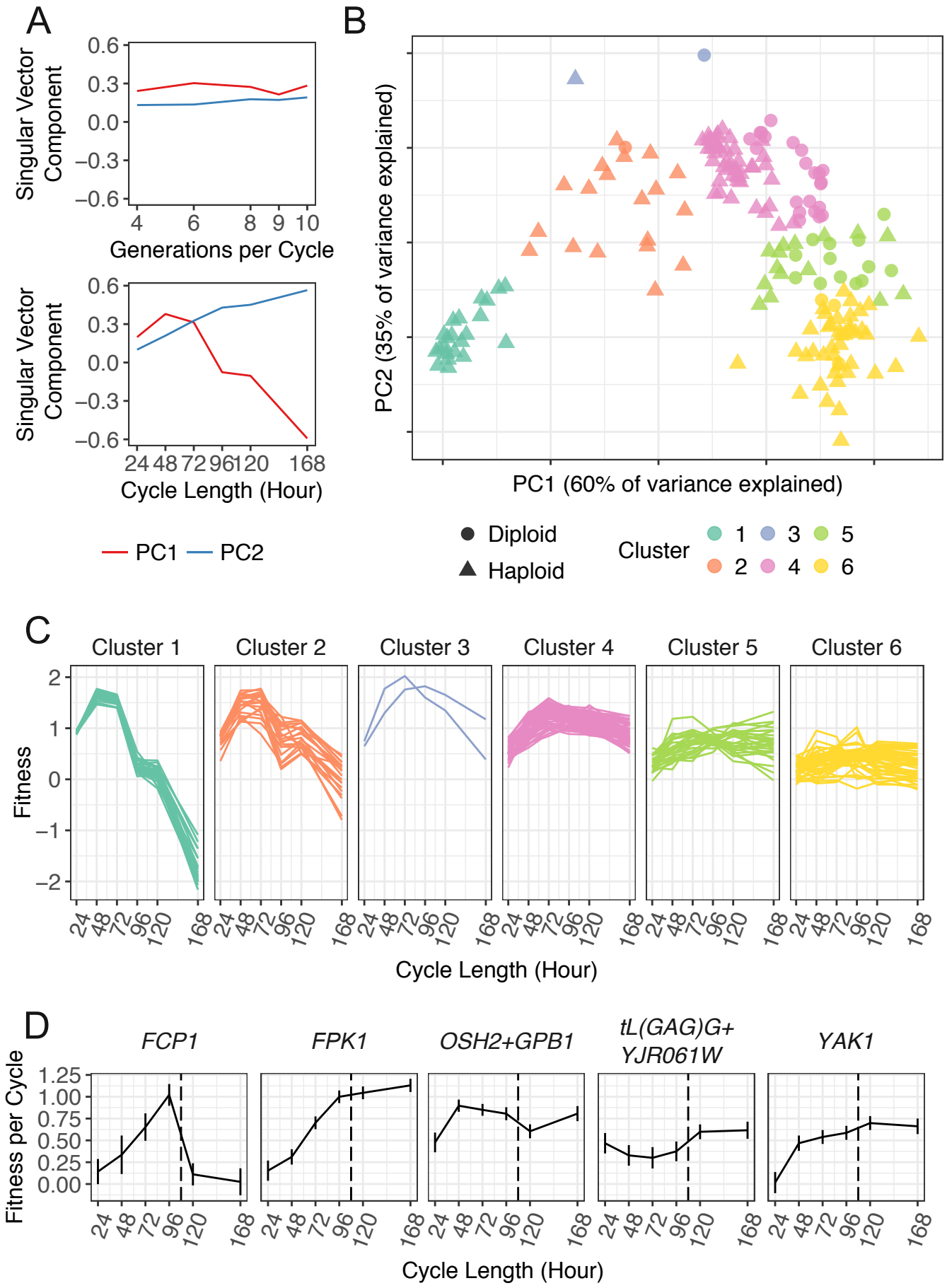
A
Singular Vector Component
0.6
0.3
0.0
−0.3
−0.6
4
6
8
9
10
Generations per Cycle
Singular Vector Component
24 48 72 96 120 168
Cycle Length (Hour)
PC1
PC2
B
PC2 (35% of variance explained)
PC1 (60% of variance explained)
Diploid
Haploid
Cluster
1
2
3
4
5
6
C
Cluster 1
Cluster 2
Cluster 3
Cluster 4
Cluster 5
Cluster 6
Fitness
Cycle Length (Hour)
D
FCP1
FPK1
OSH2+GPB1
tL(GAG)G+ YJR061W
YAK1
Fitness per Cycle
1.25
1.00
0.75
0.50
0.25
0.00
Cycle Length (Hour)

Figure S6: Singular vectors in the PCA and clustering analysis using PCA, Related to Figure 7

(A) Singular vectors corresponding to PC1 and PC2 in the PCA using adaptive haploids and high fitness diploids. For the convenience of comparing between PC1 and PC2, we plot the negative vector of PC1 (-PC1) in this figure. Top: singular vector components corresponding to conditions with varying dilution. Bottom: singular vector components corresponding to conditions with varying growth cycle. Singular vector of PC1 corresponds mostly to curvature of varying growth cycle experiments; singular vector of PC2 corresponds to its slope.

(B) Lineages are grouped into 6 clusters by applying hierarchical clustering to lineages' PCs.

(C) Fitness trajectories of adaptive haploids and high fitness diploids from each cluster, under varying cycle length conditions.

(D) Cluster 5 and 6 contain lineages that behave differently from the majority of the nutrient response pathway mutants. The fitness trajectories of five clones from clusters 5 and 6 are shown here. *OSH2*+*GPB1* and *FPK1* mutants are from cluster 5. *FCP1, tL(GAG)G*+YJR061W and *YAK1* mutants are from cluster 6. The vertical dashed line separates Batch C and Batch D of experiments (see STAR Methods). *GPB1* and *YAK1* are Ras/PKA pathway genes.

Strain Name	Barcode ID	Mutated Gene	Mutation Type	Ploidy
CYR1	43692	*CYR1*	missense_variant	Haploid
Diploid	3920	N/A	N/A	Diploid
GPB1	75669	*GPB1*	stop_gained	Haploid
GPB2	7774	*GPB2*	stop_gained	Haploid
IRA1-MISSENSE	43361	*IRA1*	missense_variant	Haploid
IRA1-NONSENSE	21967	*IRA1*	stop_gained	Haploid
IRA2	6582	*IRA2*	missense_variant	Haploid
KOG1	24737	*KOG1*	missense_variant	Haploid
PDE2	20967	*PDE2*	stop_gained	Haploid
RAS2	11430	*RAS2*	missense_variant	Haploid
SCH9+Diploid	14485	*SCH9*	missense_variant	Diploid
TOR1	21543	*TOR1*	missense_variant	Haploid
WT	304935	N/A	N/A	Haploid

Table S1: Strain information of twelve evolved strains measured in monocultures and high-resolution pairwise competition assays, Related to Figures 1 and 2

Note that strain *IRA1-NONSENSE*, *RAS2* and *SCH9+Diploid* carry additional mutations in genes not listed in this table (see Data S4 for details).

Measurement Group	Name	Number of parallel technical replicates	Growth time per cycle	Inoculated cells per cycle	Approximate generations per cycle
Batch A	Generations per cycle - 4	3	40h	8e+8	4
Batch A	Generations per cycle - 6	3	44h	2e+8	6
Batch A	Generations per cycle - 8 / EC	3	48h	5e+7	8
Batch B	Generations per cycle - 8 / EC	3	48h	5e+7	8
Batch B	Generations per cycle - 9	3	50h	2.5e+7	9
Batch C	Cycle Length - 1 day	3	24h	5e+7	8
Batch C	Cycle Length - 2 days / EC	2	48h	5e+7	8
Batch C	Cycle Length - 3 days	3	72h	5e+7	8
Batch C	Cycle Length - 4 days	3	96h	5e+7	8
Batch D	Cycle Length - 5 days	3	120h	5e+7	8
Batch D	Cycle Length - 6 days	3	144h	5e+7	8
Batch D	Cycle Length - 7 days	3	168h	5e+7	8

Table S2: Detailed parameters of measurement conditions, Related to Figure 3

Supplemental References

1. Venkataram, S., Dunn, B., Li, Y., Agarwala, A., Chang, J., Ebel, E.R., Geiler-Samerotte, K., Hérissant, L., Blundell, J.R., Levy, S.F., *et al.* (2016). Development of a Comprehensive Genotype-to-Fitness Map of Adaptation-Driving Mutations in Yeast. Cell *166*, 1585–1596.e22.